

# Hardware Implementation of an AIS-Based Optimal Excitation Controller for an Electric Ship

Chuan Yan, *Student Member, IEEE*, Ganesh Kumar Venayagamoorthy, *Senior Member, IEEE*, and Keith Corzine, *Senior Member, IEEE*

**Abstract**—The operation of high energy loads on the Navy's future electric ships will cause disturbances to the main bus voltage and impact the operation of the rest of the power system. This paper describes an online design and laboratory hardware implementation of an optimal excitation controller using an artificial immune system (AIS)-based algorithm. The AIS algorithm, a clonal selection algorithm (CSA), is used to minimize the effects of pulsed loads by improved excitation control and reduce the requirement on energy storage device capacity. The CSA is implemented on the MSK2812 DSP hardware platform. A comparison of CSA and the particle swarm optimization algorithm is presented. Both simulation and hardware measurement results show that the CSA-optimized excitation controller provides effective control of a generator's terminal voltage during pulsed loads, restoring and stabilizing it quickly.

**Index Terms**—Clonal selection algorithm (CSA), electric ship, optimal excitation controller, particle swarm optimization (PSO), pulsed loads.

## I. INTRODUCTION

THE NAVY'S future electric ship power system is based on the integrated power system (IPS) architecture consisting of power generation, propulsion systems, hydrodynamics, and dc zonal electric distribution system [1]. In order to maintain power quality in IPS, immediate energy storage devices with their corresponding charging systems are proposed to make the pulsed power required compatible with the supply system [16]. However, this will increase the system weight and volume. To some extent, the generator field excitation control can be used along with energy storage to maintain the system voltage. The excitation control is one of the most effective and economical techniques for stabilizing the terminal voltage of the synchronous generators. An optimally tuned excitation system offers benefits in overall operating performance during transient conditions caused by system faults, disturbance, or

motor starting [2]. In order to optimize them, many algorithms are extended to the design of the optimal excitation controller for the synchronous generators. Two methods are predominantly used, one being the pole-placement method and the other being the cancellation approach [2], [3]. However, transfer function and parameters of machines are needed, and they are not optimally oriented. In [4], Lyapunov's direct method has been used to optimize the excitation controller. However, again, machine parameters are needed.

Recently, computational intelligence methods have been widely used in optimizing excitation controllers such as fuzzy set theory [5], particle swarm optimization (PSO) theory [6], [7], and online trained neurocontroller [8], [9], all of which have good performance at maintaining the terminal voltage. In [7], a comparison of a PSO-based automatic voltage regulator (AVR) and a genetic algorithm (GA)-based AVR is made. Moreover, it is clearly shown from the results that the PSO-based AVR has more robust stability and efficiency and can solve the searching and tuning problems of excitation system more easily and quickly than the GA method. In [10], a comparison of differential evolution-based PSO, clonal selection algorithm (CSA), small-population-based particle swarm optimization, and population-based incremental learning for power system stabilizer design is made. The results show that CSA consistently performs better than the other three algorithms. Furthermore, in [7] and [10], all comparison results were obtained by Matlab simulation. Therefore, it is necessary to study the performance of CSA-based excitation system and hardware implementation comparison.

Artificial immune system (AIS) can be defined as computational systems that are inspired by theoretical immunology. CSA is a member of the family of AIS techniques. In the past few years, CSA has been gradually used to solve the optimal control problems [14]–[19]. In this paper, an online CSA-based optimal excitation controller for the electric ship is implemented on the MSK2812 DSP hardware platform to minimize voltage deviations when high-power pulsed loads are directly powered from the dc side, exploring the possibility of reduced energy storage. The hardware results show that the online CSA-based controller improves the dynamic performance of the synchronous generator with stability. In addition, PSO [11] has been implemented, and comparison with CSA in terms of performance and computational complexity for real-time tuning is discussed in this paper.

This paper is organized as follows: A description of a laboratory power system model for an electric ship and its hardware setup is provided in Section II. Section II gives a PSO-based

Manuscript received November 16, 2009; revised April 27, 2010; accepted July 13, 2010. Date of publication January 6, 2011; date of current version March 18, 2011. Paper 2009-IACC-083.R1, presented at the 2008 Industry Applications Society Annual Meeting, Edmonton, AB, Canada, October 5–9, and approved for publication in the IEEE TRANSACTIONS ON INDUSTRY APPLICATIONS by the Industrial Automation and Control Committee of the IEEE Industry Applications Society. This work was supported by the U.S. Office of Naval Research through the 2007 Young Investigator Award (The Intelligent All Electric Ship Power System) under Contract N00014-07-1-0806.

C. Yan is with the Trane Residential Solutions, Tyler, TX 75707 USA (e-mail: chuan.yan@irco.com).

G. K. Venayagamoorthy and K. Corzine are with the Real-Time Power and Intelligent Systems Laboratory, Missouri University of Science and Technology, Rolla, MO 65409 USA (e-mail: gkumar@ieee.org; corzinek@mst.edu).

Color versions of one or more of the figures in this paper are available online at <http://ieeexplore.ieee.org>.

Digital Object Identifier 10.1109/TIA.2010.2103540

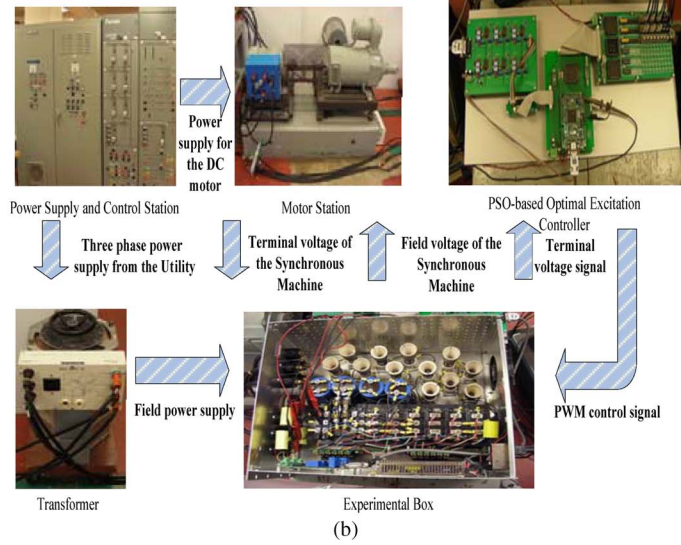
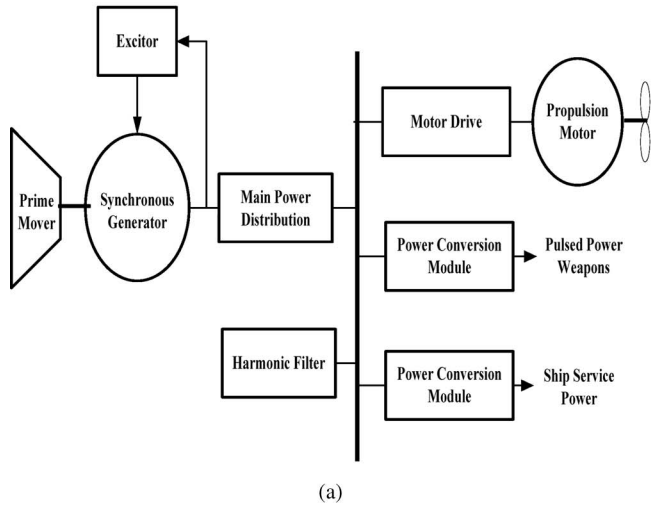


Fig. 1. (a) Laboratory hardware model and (b) setup of an IPS of an electric ship.

optimal excitation controller design. Section III provides a detailed description of the DSP-based hardware implementation of a real-time CSA algorithm for optimal excitation controller design. Section IV presents the experimental results and some discussions on the CSA algorithm in comparison to PSO. Finally, the conclusion is given in Section V.

## II. LABORATORY POWER SYSTEM MODEL FOR THE ELECTRIC SHIP POWER SYSTEM

### A. Electric Ship Integrated Power System

The power system of the all-electric ship mainly consists of four parts: prime movers, advanced propulsion induction motors, dc zonal distribution loads, and other auxiliary loads which are shown in Fig. 1. All prime mover power is first converted into electric power, and then, it is distributed and allocated between propulsion, pulsed power weapons, ship service power, and other electrical loads, as required. In the laboratory setup, these four parts are separately implemented. More details are given hereinafter on the individual modules in the hardware setup as follows.

### B. Power Generation

The DDG-1000 electric ship power system architecture consists of four gas turbine-generator sets. Two main 36 MW and two auxiliary 4 MW generator sets generate a total of 80 MW of electric power [12]. The IPS is a symmetrical system, and modeling of one of the pairs is sufficiently enough to study the excitation control. In the laboratory setup (Fig. 1), a small-scale power generation system is used to emulate the gas turbine-generator sets of the electric ship. This small-scale system consists of a three-phase 60-Hz 3.7-kVA synchronous generator and a 15-kW dc motor to supply mechanical torque for the synchronous generator. The rated line-to-line voltage and speed of the generator are 230 V and 1800 r/min, respectively. Parameter of the synchronous generator is shown in Table I. For the scaled

TABLE I  
SYNCHRONOUS MACHINE RATINGS AND PARAMETERS

Power 3.7 kVA		field voltage 150 VMAX	
voltage 230 V		field current 1.05 A	
rated current 6.28 A		speed 1800 RPM	
frequency 60 Hz		$N_s/N_{fd} = 0.0271$	
$r_s = 0.38 \Omega$	$L_{ls} = 1.12 \text{ mH}$	$L_{mq} = 29.4 \text{ mH}$	$L_{md} = 39.3 \text{ mH}$
$r'_{fd} = 0.11 \Omega$	$L'_{fd} = 1.5 \text{ mH}$	$r'_{kd1} = 128 \Omega$	$L'_{lkd1} = 7.90 \text{ mH}$
$r'_{kd2} = 1.77 \text{ m}\Omega$	$L'_{lkd2} = 4.83 \text{ mH}$	$r'_{kq1} = 5.07 \Omega$	$L'_{lkq1} = 4.21 \text{ mH}$
$r'_{kq2} = 1.06 \Omega$	$L'_{lkq2} = 3.50 \text{ mH}$	$r'_{kq3} = 0.447 \Omega$	$L'_{lkq3} = 26.2 \text{ mH}$

down laboratory model, the propulsion load and pulsed loads of the IPS in the electric ship are reduced in magnitude.

### C. Propulsion System

In the notional electric ship, a propulsion system consists of a transformer, a rectifier, an inverter, and a propulsion motor [1]. In the laboratory setup, a 2.65-kW resistive load on the dc side is used to simulate the load impact of the propulsion motors on the IPS.

### D. DC Zone Distribution Load

In the electric ship power system, there are many different pulsed loads of various energy demands and durations [12]. In the laboratory setup, a diode rectifier is used along with a passive filter to realize the power conversion module, and three insulated-gate bipolar transistor (IGBT)-controlled resistive loads are used to represent the three loads of different energy demand on the dc side (2.65, 5.29, and 5.29 kW, respectively). By switching on different IGBTs over time, the effects of a time-varying power profile which represent pulse-power consuming loads can be studied [1]. Compared with pulsed loads, the impact of other auxiliary load to the IPS can be neglected.

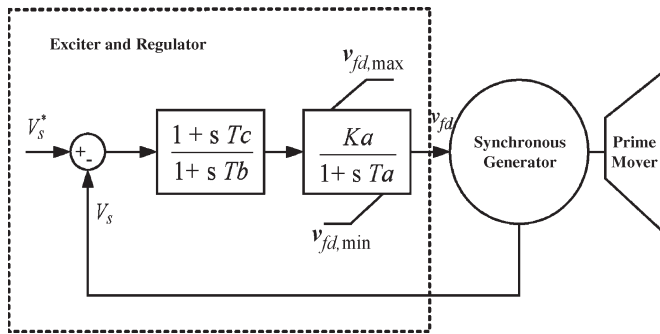


Fig. 2. Simple functional block diagram for synchronous machine excitation control system.

E. Excitation System

The synchronous generator excitation system includes a terminal voltage transducer and load compensator, excitation control elements, and an exciter [13]. Since the proposed excitation system is simplified, some parts, such as the power system stabilizer and under-excitation limiter, are not considered. A simple functional block diagram for excitation controller is shown in Fig. 2.

In this case, the key element in the design of an optimal excitation controller is finding the controller parameters ( $K_a$ ,  $T_a$ ,  $T_b$ , and  $T_c$ ) to provide optimal performance during pulsed loads. As shown in Fig. 2,  $V_s^*$  is the rms terminal voltage reference of the synchronous generator and  $V_s$  is the measured value. The rms line-to-neutral terminal voltage is calculated in terms of instantaneous quantities using

$$V_s = \frac{\sqrt{v_{as}^2 + v_{bs}^2 + v_{cs}^2}}{\sqrt{3}} \quad (1)$$

In the laboratory setup, the excitation controller consists of a sensor board, an analog-to-digital (A/D) conversion board, an MSK2812 DSP board consisting of the TMS320F2812 processor, and a digital-to-analog (D/A) conversion board. The A/D conversion board receives the terminal voltage signal from the sensor board and outputs a digital signal to the central controller. The D/A conversion board receives pulsewidth modulation (PWM) signals from the central controller and sends signals to the IGBTs. The field of the synchronous generator is connected with a four-quadrant PWM dc drive supplied by 200-V dc.

III. CSA-BASED OPTIMAL EXCITATION CONTROLLER ON LINE DESIGN

The clonal selection algorithm is a biologically motivated computational intelligence algorithm developed by Castro and Zuben in 2001 [14]. Clonal selection principle-based immune response is generated when a nonself antigenic pattern is recognized by the B cells (antibodies), as is explained in [14]. Just like many other heuristic optimization algorithms, CSA is known as an evolutionary strategy capable of solving complex machine learning and pattern recognition tasks by adopting the clonal operator. CSA can handle complex optimization problems, finding global solutions with fast con-

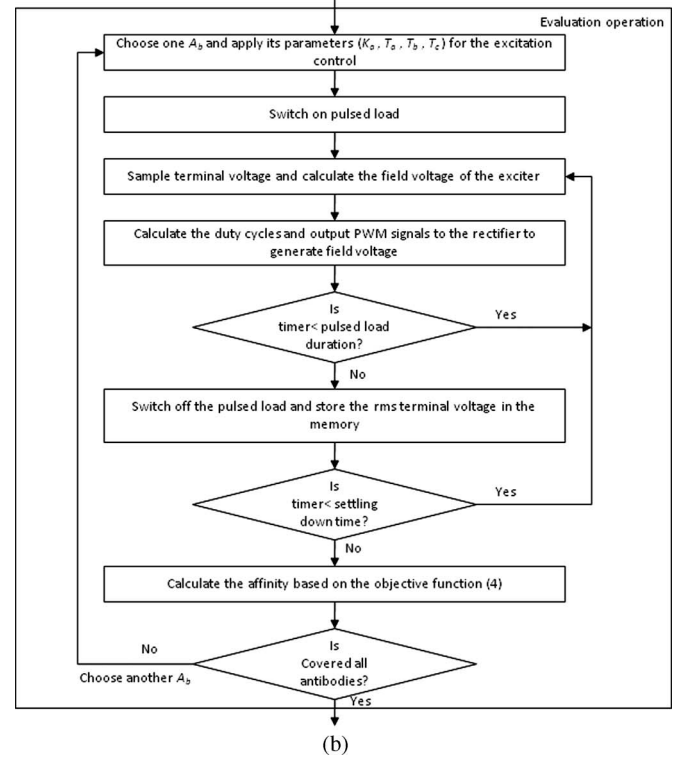
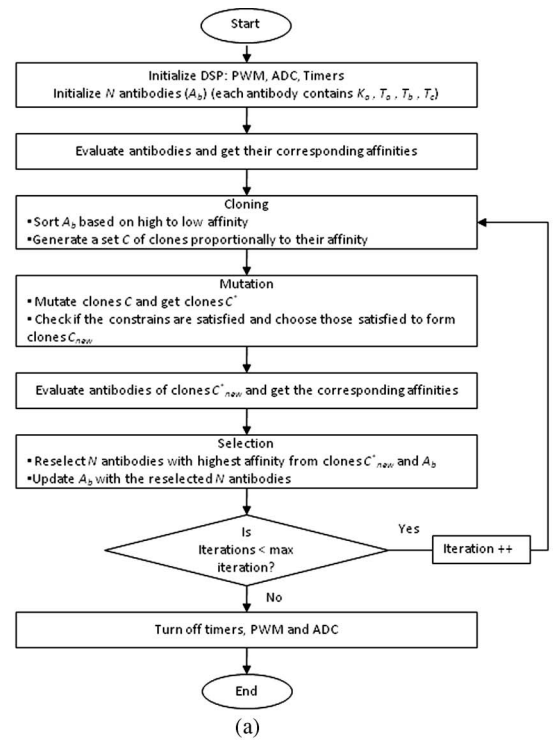


Fig. 3. Flowcharts of the (a) CSA-based optimal excitation controller design and (b) evaluation operation.

vergence speeds, particularly for functions of multimodal and highly combinatorial nature [15]–[19]. The detailed operation of CSA is illustrated in the flowchart depicted in Fig. 3, and the main steps are briefly explained as follows. In this paper, by online, it means that the parameters of excitation controller are determined via several runs/iterations of CSA algorithm using the actual hardware in Fig. 1(b).

*Initialization:* A population  $N$  of antibodies ( $A_b$ ) is randomly initialized. Since there is no explicit antigen population ( $A_g$ ) to be recognized as there would be in a biological system, the objective function serves as the  $A_g$  and needs to be minimized or kept at zero. In order to keep the hardware overhead within real-time constraints,  $N$  is selected to be 20. The initialization range for parameters is obtained by trial and error which can make the system stable. Specifically,  $K_a$  ranges from 100 to 7000;  $T_a$  ranges from 0 to 5; and  $T_b$  and  $T_c$  range from 0 to 10.

*Evaluation:* In the excitation control loop of Fig. 2, the proportional gain  $K_a$  and time constants  $T_a$ ,  $T_b$ , and  $T_c$  have to be carefully selected to provide satisfactory performance under normal and pulsed-load conditions. The objective of the CSA algorithm is to find these parameters in order to restore and stabilize the terminal voltage quickly, particularly, after pulsed loads of different magnitudes and durations are experienced by the IPS.

Most objective functions used for excitation controller design in the literature involve settling time, rise time, and overshoot. In this paper, the objective function associated with the AVR performance is obtained by calculating the transient response area (2) [20], [21]. This can be used as a fitness function to guide the PSO design process to minimize the time response characteristics such as rise time, overshoot, and settling time

$$\text{Fitness} = \frac{1}{2} \sum_{k=1}^n \left\{ \sqrt{[V_s^* - V_s(k)]^2 + [V_s^* - V_s(k+1)]^2} \right\} \Delta t \quad (2)$$

where

- $V_s^*$  reference terminal voltage value;
- $k$  sampling instant;
- $\Delta t$  sampling interval;
- $V_s$  measured terminal voltage.

Due to the high computational overhead involved in computing the square root function on a DSP, (2) is modified to (3) for controller design. The term  $(k\Delta t)$  is a weighting factor that puts an increasing penalty as oscillations persist for a longer time, thus guiding the CSA design approach to minimize the settling time of the system oscillations in addition to the maximum overshoot after a disturbance

$$\text{Fitness} = \frac{1}{2} \sum_{k=1}^n \left\{ [V_s^* - V_s(k)]^2 + [V_s^* - V_s(k+1)]^2 \right\} (k \cdot \Delta t) \Delta t. \quad (3)$$

According to the clonal selection principle [14], the affinity maturation process is from producing low-affinity  $A_b$ 's to high-affinity  $A_b$ 's. The smaller the system oscillation is, the larger the affinity is. Therefore, the affinity for use in the CSA is evaluated by (4)

$$\text{Affinity}_i = \frac{1}{1 + \text{Fitness}_i} \quad (4)$$

where  $i$  is the number of  $A_b$  and  $\text{Fitness}_i$  is the fitness of the  $i$ th  $A_b$ .

Since the fitness value is always positive, the range of affinity value is normalized over the interval [0, 1].

In the laboratory setup, the sampling window is 1 s, starting from the time when the pulsed load is removed. The sampling period is 2 ms, and a total of  $n = 500$  sample points are collected.

*Cloning:* All antibodies are ranked based on affinity from high to low. A set  $C$  of clones are generated proportionally to the affinities of the  $A_b$ 's in the population given by

$$N_c = \sum_{\# = 1}^r \text{round} \left( \frac{\beta \times N}{r\#} \right) \quad (5)$$

where

- $N_c$  number of clones in each set;
- $\beta$  multiplying factor;
- $r$  number of selected ranks;
- $r\#$  1 for highest affinity, 2 for second highest affinity, and so on.

In [14], [16], it is clear that a high value of  $\beta$  can give a better convergence. However, the number of function evaluations will also increase correspondingly. In this paper,  $\beta$  and  $r$  are set to be 0.5 and 5, respectively, which can give a good convergence. In this case, the population of matured clones is 23, which is close to  $N_c$ . Therefore, the number of function evaluations for CSA is close to the one for PSO, which gives a fair comparison.

*Mutation:* The mutation rate is selected to be proportional to individual affinities as given in

$$\alpha = e^{-\rho \times f} \quad (6)$$

where

- $\alpha$  mutation rate;
- $\rho$  decay factor of the mutation rate;
- $f$  antigenic ( $A_g$ ) affinity.

The tradeoff between the mutation rate  $\alpha$  and the antigenic affinity  $f$  is shown in [14]. A small decay factor gives large mutation and vice versa. A large mutation rate means more exploration, while a small mutation rate results in exploitation and vice versa. In this paper, the decay factor is set to be one. The antigenic affinity and mutation rate are both normalized over the interval [0, 1]. The process of mutation is given by (7) developed in [17]

$$C^* = C + \alpha \times \text{randn} \times C + \alpha \times \text{randn} \times (C - A_{\text{bbest}}) \quad (7)$$

where  $C^*$  is the mutated clones and  $A_{\text{bbest}}$  is the antibody with highest affinity.

In the laboratory setup, the excitation controller parameters  $K_a$ ,  $T_a$ ,  $T_b$ , and  $T_c$  to be used for fitness evaluation have to be within a range of values. This is necessary to ensure that the electrical machine remains stable. Antibodies that satisfy this constraint which is the same with initialization range are referred to as feasible antibodies in the set  $C^*$  (obtained from operation using (7)) and form a new set  $C_{\text{new}}^*$ .

*Selection:* Reselect  $N$  antibodies with highest affinity from clones  $C^*$  and  $C_{\text{new}}^*$  and update  $A_b$ .

The CSA algorithm parameter setting is shown in Table II.

TABLE II  
SPECIFICATION FOR CSA AND PSO ALGORITHM PARAMETERS

Decay factor of mutation rate $\rho$	1
Multiplying factor $\beta$	0.5
Total number of antibodies	20
Number of selected highest $A_b$	5

TABLE III  
PULSED-LOAD TRAINING AND TESTING SETS

Duration \ Pulsed load	100 ms	200 ms	400 ms	1000 ms
2.65 kW	Test	Test	Test	Test
5.29 kW	Test	Test	Test	Train
7.94 kW	Test	Test	Train	
13.23 kW	Test	Test		

The pulsed-load magnitudes and duration used in controller development and testing are shown in Table II. Two pulsed loads, which are labeled “Train” in Table III, are applied to serve as antigens. After the optimal parameters have been obtained, other eleven different pulsed loads are used to verify the performance of the optimal controller, which are labeled as “Test.”

#### IV. PSO-BASED OPTIMAL EXCITATION CONTROLLER DESIGN

PSO is a swarm intelligence technique (a search method based on nature-inspired systems), which is widely used in electric power systems [11]. It is an efficient method for solving one or more large-scale nonlinear optimization problems [7]. The system initially has a population of random particles which are given some random positions and velocities in the search space. The particles have memory which is used to keep track of their previous best position local best ( $P_{best}$ ) and the corresponding fitness. The swarm has a memory which is used to keep track of the best value of all  $P_{best}$ . The search process is aimed at accelerating each particle toward its  $P_{best}$  and the swarm’s global best ( $G_{best}$ ). The velocity and position update equations of the particles are given by

$$v_i(j+1) = w \cdot v_i(j) + c_1 \cdot R_1 \cdot (P_{best}(j) - x_i(j)) + c_2 \cdot R_2 \cdot (G_{best} - x_i(j)) \quad (8)$$

$$x_i(j+1) = x_i(j) + v_i(j+1) \quad (9)$$

where  $w$  is the inertia constant,  $c_1$  and  $c_2$  are two positive numbers referred as the cognitive and social acceleration constants, and  $R_1$  and  $R_2$  are two random numbers with uniform distribution in the interval [0, 1].

The detailed procedure for the development of optimal excitation controllers is given as follows.

*Initialization:* Randomly initialize a population  $N$  of particle positions and velocity. To have a fast PSO search performance, in the laboratory setup,  $N$  is set to be 20, and the values of  $w$ ,  $c_1$ , and  $c_2$  are kept fixed at 0.8, 2.0, and 2.0 [11].

*Evaluation:* The objective of the PSO algorithm is to find optimal parameters in order to restore and stabilize the terminal

voltage quickly, particularly after pulsed loads of different magnitude and duration. The fitness function is using (3).

*Update:* The position and velocity of the  $i$ th particle is updated using (8) and (9).

#### V. RESULTS

The CSA and PSO algorithms for comparison have been implemented on two platforms: 1) Matlab/Simulink simulation and 2) hardware implementation using the MSK2812 DSP controlling the laboratory setup shown in Fig. 1. The comparison is made under the following conditions: same value and dimension of initialized antibodies or particles and same number of allowed generations/iterations for searching the optimal parameters under the same constrains. By doing this, the influence introduced by the randomly updating process could be minimized.

##### A. MATLAB/SIMULINK-Based System

In this paper, a generator with parameters shown in Table I and power system in Fig. 1(b) is built in Matlab/Simulink using SimPowerSystem toolbox. A variable load is used to simulate the propulsion loads. The load is gradually changing from 1.65 to 2.65 kW during the pulsed load in order to simulate ship acceleration. In this case, the operating point is changing during the pulsed load, which makes the simulated operating conditions similar to the ship’s real operation conditions. A pulsed load of 5.29 kW with 0.75-s duration is used for tuning controller parameters using CSA and PSO shown in Sections III and IV, respectively.

For a more extensive comparison, a pole placement method [2] is also applied in this study. A first-order generator model is obtained using the equations in [22], [23] with a gain taken as 0.7012 and the time constant taken as 0.274 while assuming negligible amortisseur effects. Voltage overshoot of at least 1%–20% is anticipated with the pole-placement method with 2-s total voltage recovery time, although its voltage rise time can be less than 1 s [2]. In this case, the range of damping ratio is from 0.456 to 0.8261 [24]. In this paper, the damping ratio is chosen to be around 0.707. Both CSA and PSO are run for 30 trials. Among these 30 trials, one best antibody and one best particle are chosen as the parameters for the CSA-based controller and PSO-based controller, respectively. In addition, the parameters obtained by pole placement, PSO, and CSA are shown in Table IV.

The average fitness of the best parameters using PSO and CSA over 100 iterations based on 30 trials is shown in Fig. 5. A statistical analysis based on standard deviation is evaluated using

$$\sigma = \sqrt{\frac{1}{n} \sum_{i=1}^n (F_i - F_{ave})^2} \quad (10)$$

where

$i$  1 for the first trial, 2 for the second trial, and so on;

$n$  total number of trials which is 30;

$F_{ave}$  average best fitness for 30 trials;

$F_i$ ,  $i$ th trial best fitness value for selected algorithm.

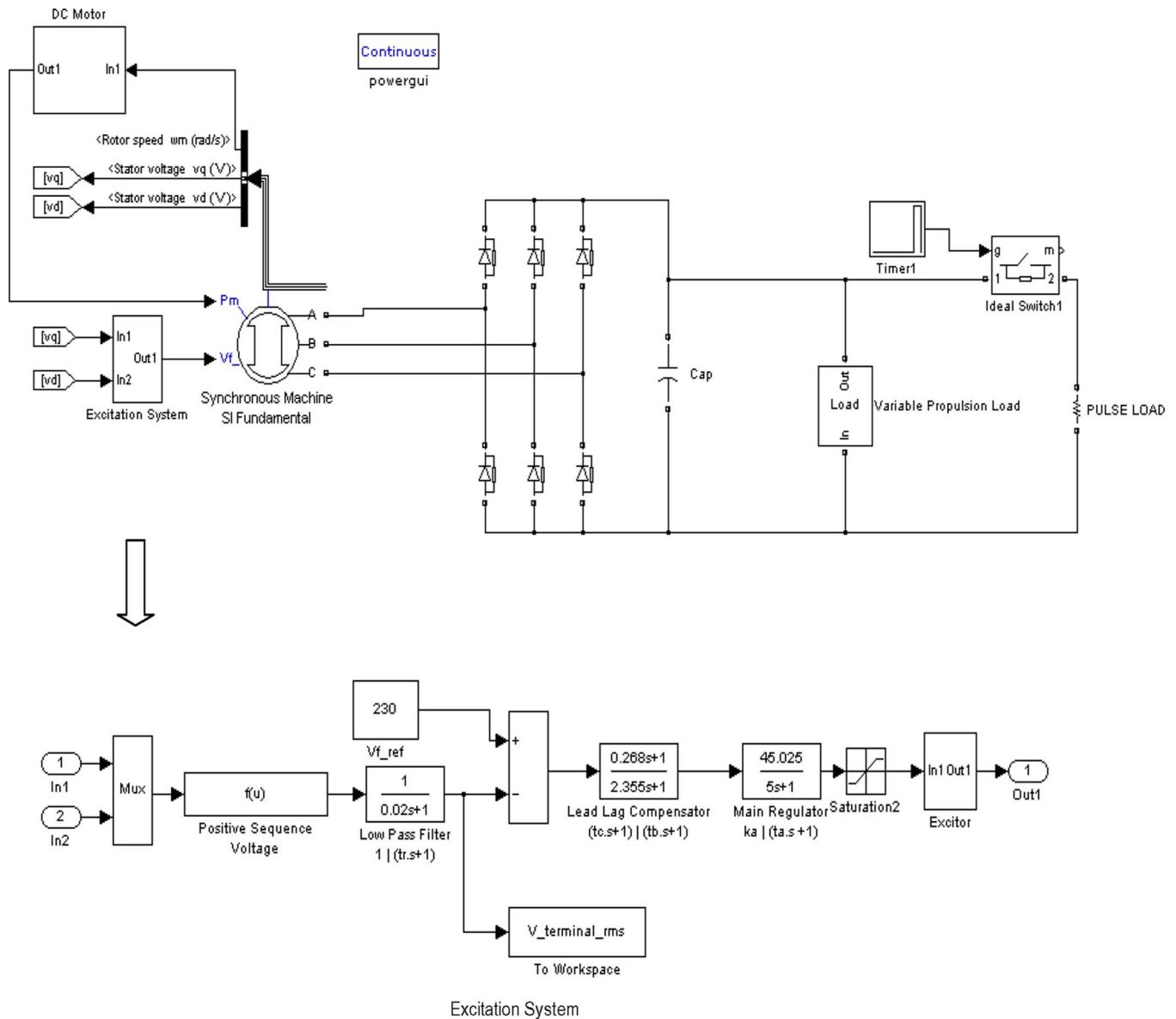


Fig. 4. Test ship power system for MATLAB/SIMULINK-based implementation.

TABLE IV  
PARAMETERS OF THE EXCITATION CONTROLLERS

	$K_A$	$T_A$	$T_B$	$T_C$
Pole-placement	885.609	0.001	2.356	0.268
PSO	398.524	0.998	0.0001	0.467
CSA	424.723	0.0001	3.084	1.056

In (10),  $\sigma$  is the standard deviation for the best solution for selected algorithm, which are 0.0317 and 0.0185 for PSO and CSA, respectively. It is clear that CSA accuracies around their corresponding best solution are higher than PSO.

A performance comparison of these three methods under 5.29-kW pulsed load with 0.75-s duration is shown in Fig. 6. In Fig. 6(a), the start-up performance comparison is shown. The

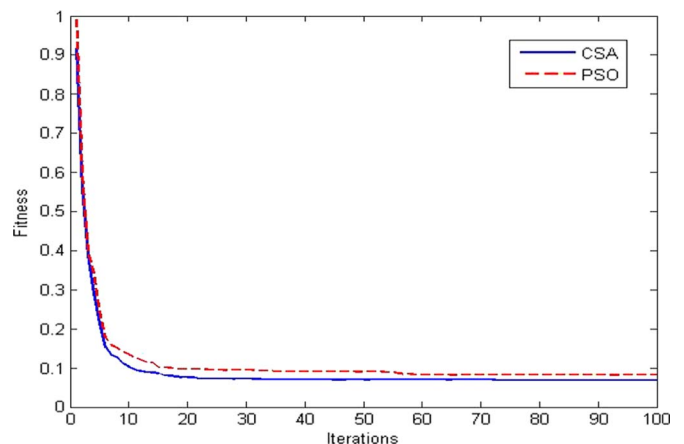


Fig. 5. Average fitness of best particle/antibody using PSO and CSA over 100 iterations based on 30 trials based on MATLAB simulation.

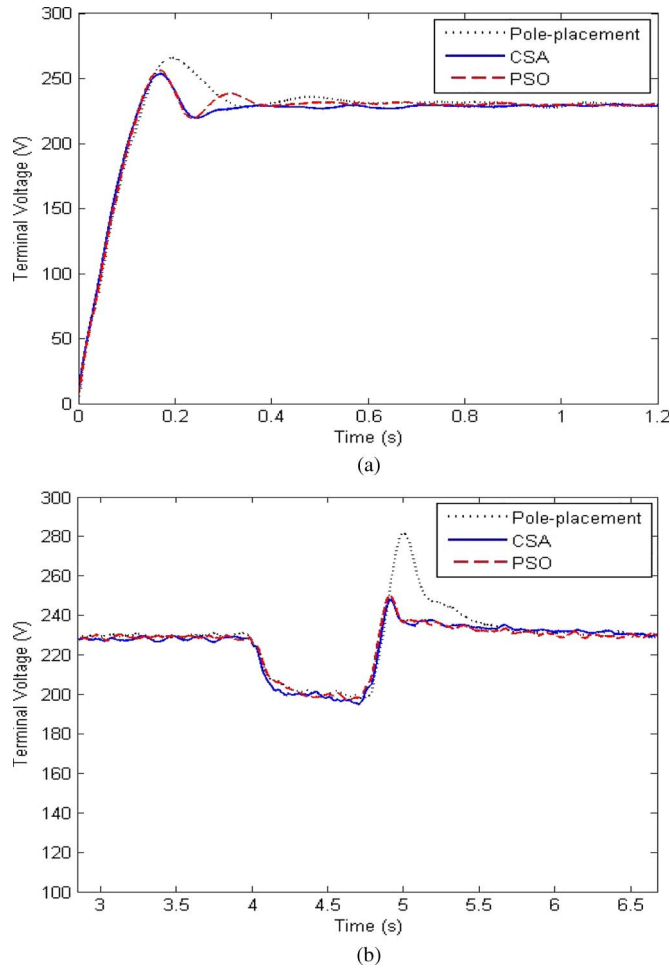


Fig. 6. Performance comparison of pole-placement-, PSO-, and CSA-based controllers based on MATLAB/SIMULINK simulation. (a) Startup performance. (b) Under 5.29 kW and 0.75-s duration pulsed load.

overshoot of pole-placement-based controller is 15.2%, and the 2% settling time is 0.52 s, which meets the design requirements. In Fig. 6(b), a performance comparison of these three methods under a 5.29 kW 0.75-s duration pulsed load is shown. It is clear that the performance of the CSA-based controller is very close to the performance of the PSO-based controller, which means that both of them have good exploitation. However, according to the fitness standard deviation value and Fig. 5, CSA has better convergence.

### B. Hardware Results

The hardware testbed is described in Section II. The CSA and PSO algorithms are implemented in a MSK2812 DSP with 150-MHz frequency.

1) *Execution Time and Convergence Characteristics*: The convergence of CSA and PSO algorithms during the search process over 40 iterations/generations based on ten trials is shown in Fig. 7.

The computational time taken by PSO and CSA using MSK2812 DSP is presented in Table V. A single generation code execution time for an  $A_b$  in CSA is nearly three times (0.064 s) that of a PSO particle (0.022 s). However, for this controller design application, when comparing the total time

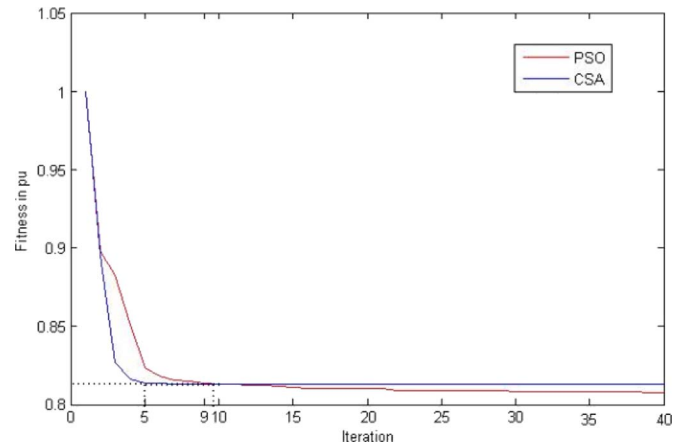


Fig. 7. Average fitness of the best particle using PSO and CSA over 40 iterations based on ten trials for hardware testbed.

TABLE V  
COMPUTATIONAL TIME TAKEN BY PSO AND CSA

	PSO	CSA
Code time for each particle/ $A_b$ (one iteration/generation)	0.022s	0.064s
Evaluation time for each particle/ $A_b$ (one iteration/generation)	7.400s	7.400s
Search time for each particle/ $A_b$ (one iteration/generation)	7.422s	7.464s

TABLE VI  
PARAMETERS OF THE EXCITATION CONTROLLERS

	$K_A$	$T_A$	$T_B$	$T_C$
PSO	4359.000	0.119	0.691	0.732
CSA	5966.908	0.158	0.019	0.045

taken by CSA and PSO algorithms, difference in the code execution time is negligible.

2) *Transient Performance*: Both CSA and PSO are running for ten times with 40 iterations every time. Among these ten trials, one best antibody and one particle are chosen as the parameters of the CSA-based controller and PSO-based controller, respectively. The parameters of excitation controller designed using CSA and PSO optimal strategies are gained given in Table VI. The comparative performances between the CSA-based controller and PSO-based controller are shown in Figs. 8–10, respectively. The comparative performance of the excitation controllers under pulsed loads (including search and test sets) is shown in Table VII. For settling time calculation, because it is hard to compare settling time if the stable range is set to be 2%, the stable range is defined as from 228 to 232 V, which is 0.87%.

Based on the analysis earlier, a comparison of CSA and PSO algorithms for excitation controller design is given in Table VIII, which includes computation complexity, storage space demand, hardware demand, convergence, and time

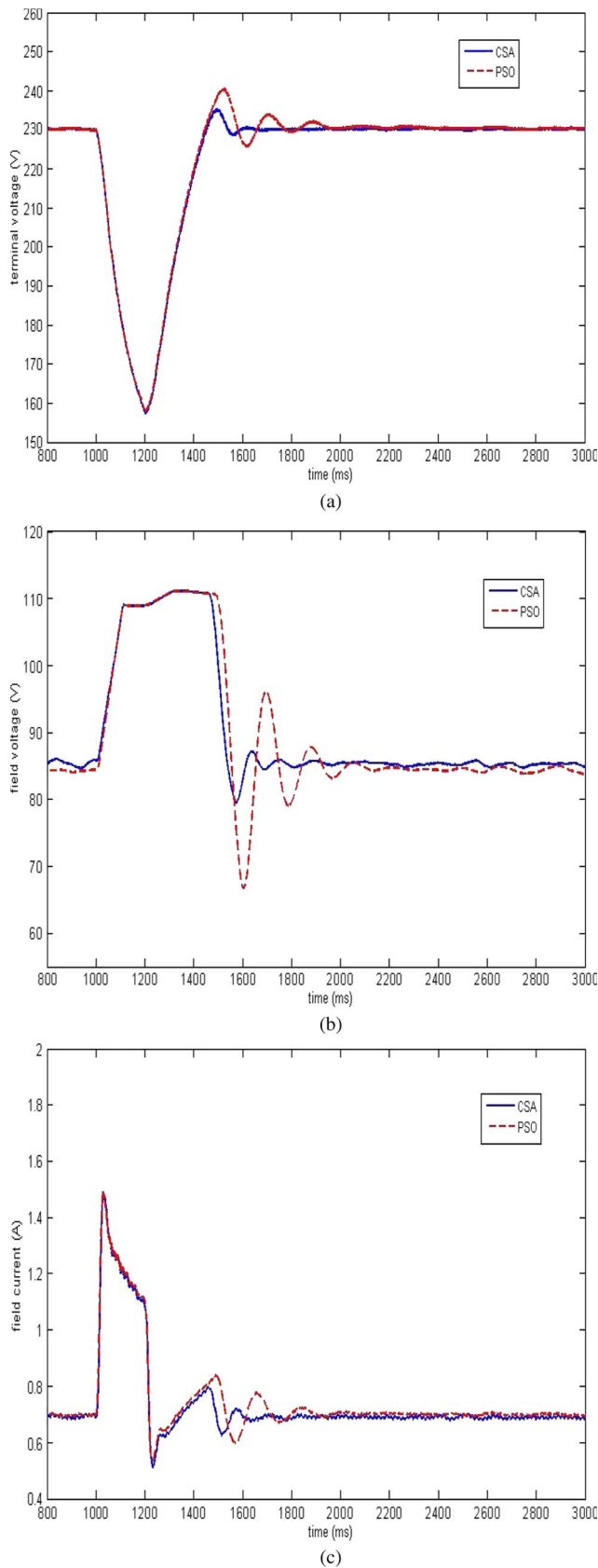


Fig. 8. Pulsed load at 5.29 kW with 0.2-s duration. (a) Terminal voltage. (b) Field voltage. (c) Field current.

consumed. With a code optimization, the clock cycles for PSO and CSA can be reduced. However, their ratio will not change significantly. Two 3-D performance analyses are shown in

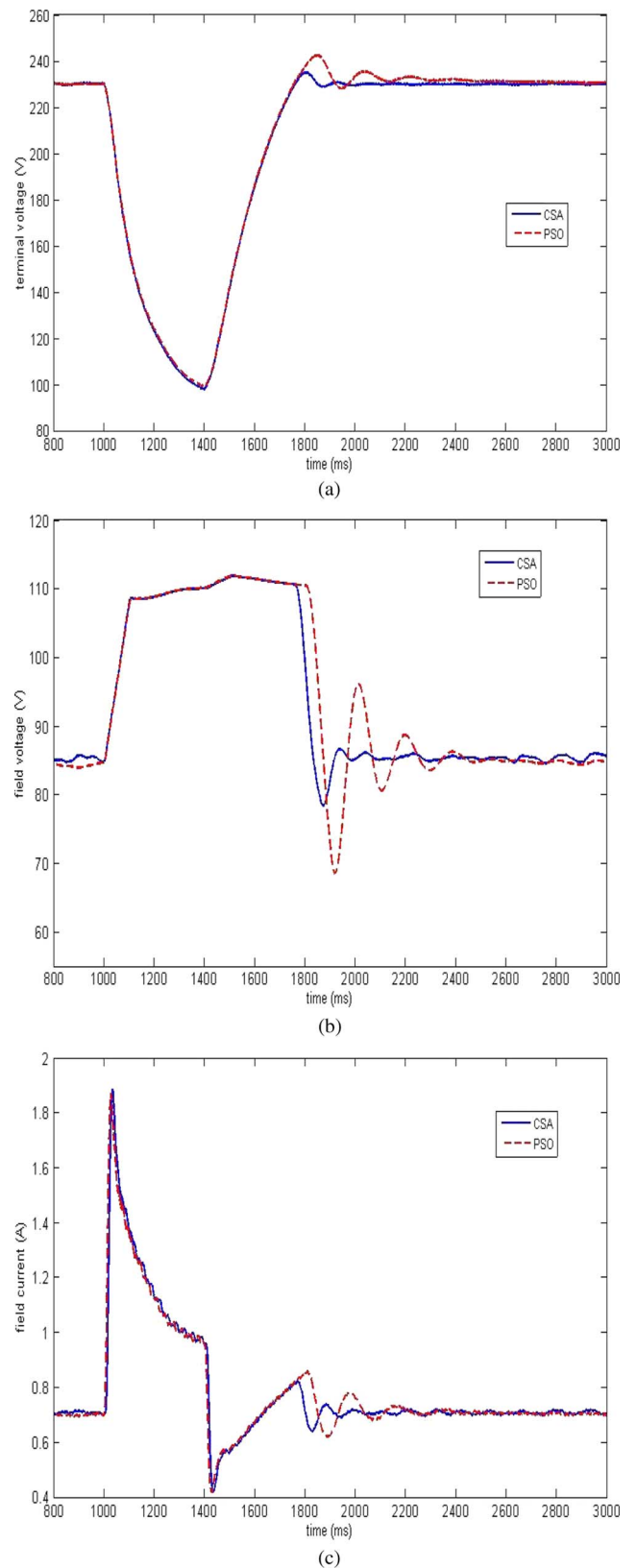


Fig. 9. Pulsed load at 7.94 kW with 0.4-s duration. (a) Terminal voltage. (b) Field voltage. (c) Field current.

Fig. 11. Fig. 11(a) shows the settling time with different pulsed-load values and durations, while Fig. 11(b) shows the overshoot performance.

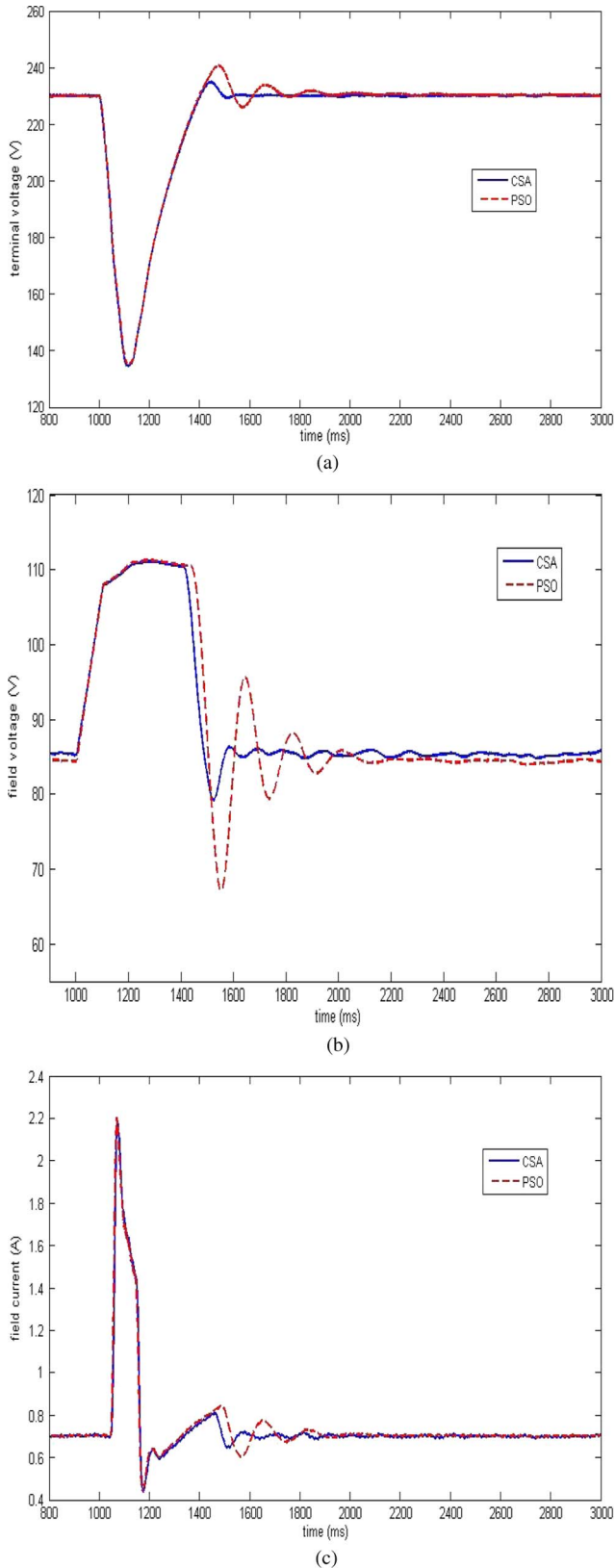


Fig. 10. Pulsed load at 13.23 kW with 0.1-s duration. (a) Terminal voltage. (b) Field voltage. (c) Field current.

## VI. CONCLUSION

An online-designed optimal excitation controller using a clonal selection algorithm, from artificial immune systems, has

TABLE VII  
COMPARATIVE PERFORMANCE OF THE EXCITATION CONTROLLERS

		Setting Time ts (s)	Maximum Overshoot (%)
Pulsed load = 2.65KW; Duration = 1s	CSA	0.26	2.31
	PSO	0.64	5.09
Pulsed load = 2.65KW; Duration = 0.4s	CSA	0.24	2.26
	PSO	0.55	5.09
Pulsed load = 2.65KW; Duration = 0.2s	CSA	0.21	2.13
	PSO	0.42	4.35
Pulsed load = 2.65KW; Duration = 0.1s	CSA	0.18	2.10
	PSO	0.32	4.30
Pulsed load = 5.29KW; Duration = 1s	CSA	0.39	2.33
	PSO	0.84	5.93
Pulsed load = 5.29KW; Duration = 0.4s	CSA	0.38	2.33
	PSO	0.78	5.22
Pulsed load = 5.29KW; Duration = 0.2s	CSA	0.33	2.31
	PSO	0.71	4.57
Pulsed load = 5.29KW; Duration = 0.1s	CSA	0.27	2.20
	PSO	0.48	4.35
Pulsed load = 7.94KW; Duration = 0.4s	CSA	0.44	2.36
	PSO	0.88	5.54
Pulsed load = 7.94KW; Duration = 0.2s	CSA	0.41	2.34
	PSO	0.80	5.09
Pulsed load = 7.94KW; Duration = 0.1s	CSA	0.33	2.22
	PSO	0.55	4.36
Pulsed load = 13.23KW; Duration = 0.2s	CSA	0.45	2.22
	PSO	0.85	5.13
Pulsed load = 13.23KW; Duration = 0.1s	CSA	0.38	2.26
	PSO	0.75	4.75

been presented in this paper. The CSA has been implemented on an MSK2812 DSP hardware platform to control a laboratory scaled down version of the Navy's future electric ship power system. This controller has advantages in that it is optimal oriented, does not require knowledge of generator parameters, and has minimal human involvement. The objective for the CSA algorithm is to minimize voltage deviations when pulsed loads are directly energized by the shipboard power system; thus reducing energy storage device capacity. In comparing CSA with PSO, both simulation and hardware results show that a CSA-based controller can restore and stabilize the terminal voltage effectively and quickly with little disturbance introduced after high-power pulsed loads are experienced.

TABLE VIII  
GENERAL COMPARISON OF CSA AND PSO ALGORITHMS FOR  
EXCITATION CONTROLLER DESIGN

	PSO	CSA
Computational functional complexity	Small, mainly “+, -, × operation”  3.3M clock cycles per particle in one iteration with 150MHz frequency	Large, contains “sorting, round, exponential, and division operation”  9.6M clock cycles per antibody in one iteration with 150MHz frequency
Computational memory requirements	Small, mainly “particles position and velocity”	Medium, “antibody, affinity, new group of antibody and affinity”
Hardware requirements	Low. Many microcontrollers such as PIC, DSP are available to be implemented on; Shallow memory requirements	High. High processing speed is needed; Memory requirements high.
Convergence	Good	Better
Algorithm code execution time	Small	Large - nearly 3 times larger than PSO

REFERENCES

- [1] L. N. Domaschk, A. Ouroua, and R. E. Hebner, “Coordination of large pulsed loads on future electric ships,” *IEEE Trans. Magn.*, vol. 43, no. 1, pp. 450–455, Jan. 2007.
- [2] K. Kim and R. C. Schaefer, “Tuning a PID controller for a digital excitation control system,” *IEEE Trans. Ind. Appl.*, vol. 41, no. 2, pp. 485–492, Mar./Apr. 2005.
- [3] K. Kim, A. Godhwani, M. J. Basler, and T. W. Eberly, “Commissioning experience with a modern digital excitation system,” *IEEE Trans. Energy Convers.*, vol. 13, no. 2, pp. 183–187, Jun. 1998.
- [4] J. Machowski, S. Robak, J. W. Bialek, J. R. Bumby, and N. AbiSamra, “Decentralized stability-enhancing control of synchronous generator,” *IEEE Trans. Power Syst.*, vol. 15, no. 4, pp. 1336–1344, Nov. 2000.
- [5] F. Zheng, Q. Wang, T. H. Lee, and X. Huang, “Robust PI controller design for nonlinear systems via fuzzy modeling approach,” *IEEE Trans. Syst., Man, Cybern. A, Syst., Humans*, vol. 31, no. 6, pp. 666–675, Nov. 2001.
- [6] A. Karimi and A. Feliachi, “PSO-tuned adaptive backstepping control of power systems,” in *Proc. IEEE Power Syst. Conf. Expo.*, Oct. 2006, pp. 1315–1320.
- [7] Z.-L. Gaing, “A particle swarm optimization approach for optimum design of PID controller in AVR system,” *IEEE Trans. Energy Convers.*, vol. 19, pp. 384–391, Jun. 2004.
- [8] G. K. Venayagamoorthy and R. G. Harley, “A continually online trained neurocontroller for excitation and turbine control of a turbogenerator,” *IEEE Trans. Energy Convers.*, vol. 16, no. 3, pp. 261–269, Sep. 2001.
- [9] G. K. Venayagamoorthy and R. G. Harley, “Two separate continually online-trained neurocontrollers for excitation and turbine control of a turbogenerator,” *IEEE Trans. Ind. Appl.*, vol. 38, no. 3, pp. 887–893, May/June 2002.
- [10] P. Mitra, C. Yan, L. Grant, G. K. Venayagamoorthy, and K. Folly, “Comparative study of population based techniques for power system stabilizer design,” in *Proc. Int. Conf. Intell. Syst. Appl. Power Syst.*, 2009, pp. 1–6.
- [11] Y. del Valle, G. K. Venayagamoorthy, S. Mohagheghi, J. C. Hernandez, and R. G. Harley, “Particle swarm optimization: Basic concepts, variants and applications in power systems,” *IEEE Trans. Evol. Comput.*, vol. 12, no. 2, pp. 171–195, Apr. 2008.
- [12] A. Ouroua, L. Domaschk, and J. H. Beno, “Electric ship power system integration analyses through modeling and simulation,” in *Proc. IEEE Elect. Ship Technol. Symp.*, 2005, pp. 70–74.
- [13] IEEE Recommended Practice for Excitation System Models for Power System Stability Studies, IEEE Standard 421.5-2005, 2006.
- [14] L. N. de Castro, F. J., and Von Xuben, “Learning and optimization using the clonal selection principle,” *IEEE Trans. Evol. Comput.*, vol. 6, no. 3, pp. 239–251, Jun. 2002.
- [15] H. Lou, C. Mao, and D. Wang, “PWM optimization for three-level voltage inverter based on clonal selection algorithm,” *IET Electric Power Appl.*, vol. 1, no. 6, pp. 870–878, Nov. 2007.
- [16] F. Campelo, F. G. Guimaraes, H. Igarashi, and J. A. Ramirez, “A clonal selection algorithm for optimization in electromagnetics,” *IEEE Trans. Magn.*, vol. 41, no. 5, pp. 1736–1739, May 2005.
- [17] X. Wang, “Clonal selection algorithm in power filter optimization,” in *Proc. IEEE Mid-Summer Workshop Soft Comput. Ind. Appl.*, Jun. 2005, pp. 122–127.
- [18] S. A. Panimadai Ramaswamy, G. K. Venayagamoorthy, and S. N. Balakrishnan, “Optimal control of class of nonlinear plants using artificial immune systems: Application of the clonal selection algorithm,” in *Proc. IEEE Int. Symp. Intell. Control*, Oct. 2007, pp. 249–254.
- [19] L. Zhang, Y. Zhong, B. Huang, J. Gong, and P. Li, “Dimensionality reduction based on clonal selection for hyperspectral imagery,” *IEEE Trans. Geosci. Remote Sens.*, vol. 45, no. 12, pp. 4172–4186, Dec. 2007.
- [20] P. Mitra and G. K. Venayagamoorthy, “An adaptive control strategy for DSTATCOM applications in an electric ship power system,” *IEEE Trans. Power Electron.*, vol. 25, no. 1, pp. 95–104, Jan. 2010.
- [21] E. R. C. Viveros, G. N. Taranto, and D. M. Falcao, “Tuning of generator excitation systems using meta-heuristics,” in *Proc. IEEE Power Eng. Soc. Gen. Meet.*, Montreal, QC, Canada, 2006, pp. 1–6.
- [22] F. P. Demello and C. Concordia, “Concepts of synchronous machine stability as affected by excitation control,” *IEEE Trans. Power App. Syst.*, vol. PAS-88, no. 4, pp. 316–329, Apr. 1969.
- [23] P. Kundur, *Power System Stability and Control*. New York: McGraw-Hill, 1993.
- [24] S. M. Sanners, *Modern Control System Theory and Design*, 2nd ed. Hoboken, NJ: Wiley-Interscience, 1998.

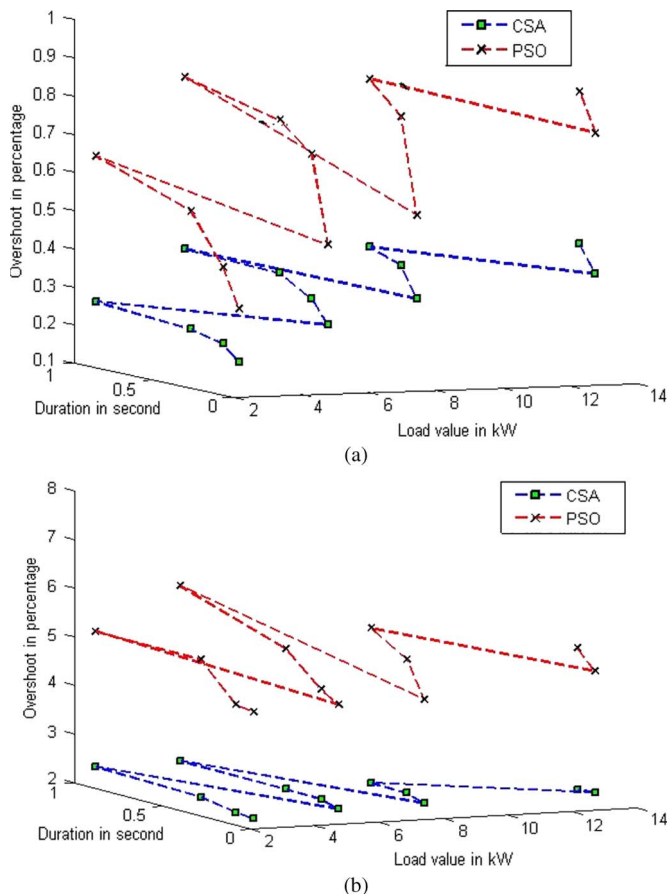
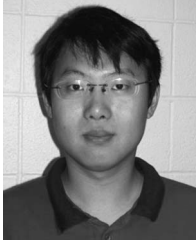


Fig. 11. (a) Settling times and (b) maximum overshoots for pulsed of different magnitudes and durations.



**Chuan Yan** (S'08) received the B.S. degree in electrical engineering from the Lanzhou University of Technology, Lanzhou, China, in 2005, the M.S. degree in electrical engineering from Chongqing University, Chongqing, China, in 2008, and the Ph.D. degree in electrical engineering from the Missouri University of Science and Technology (Missouri S&T), Rolla, in 2010.

He was a Postdoctoral Fellow with Real-Time Power and Intelligence Systems Laboratory, Missouri S&T, in 2010. He is currently a Senior

Power Electronics Engineer with Trane Residential Solutions, Tyler, TX. His research interests include motor drives, electric machinery analysis, and computational algorithms for power system stability and control.



**Ganesh Kumar Venayagamoorthy** (S'91–M'97–SM'02) received the Ph.D. degree in electrical engineering from the University of Natal, Durban, South Africa, in February 2002.

He is currently an Associate Professor of electrical and computer engineering and the Founder and Director of the Real-Time Power and Intelligent Systems Laboratory, Missouri University of Science and Technology (Missouri S&T), Rolla. He was a Visiting Researcher with ABB Corporate Research, Sweden, in 2007. His research interests are in the

development and applications of advanced computational algorithms for real-world applications, including power system stability and control, smart-grid applications, sensor networks, and signal processing. He has published two edited books, six book chapters, and over 85 refereed journal papers and 280 refereed conference proceeding papers.

Dr. Venayagamoorthy has been involved in the leadership and organization of many conferences including the 2011 IEEE Symposium of Computational Intelligence Applications in Smart Grid, being the Chair, and the 2008 IEEE Swarm Intelligence Symposium (St. Louis, U.S.), being the General Chair. He is currently the Chair of the IEEE Power Engineering Society (PES) Working Group on Intelligent Control Systems, the Chair of the IEEE Computational Intelligence Society Task Force on Smart Grid, the Chair of the IEEE PES Intelligent Systems Subcommittee, and the Chapter Chair of the IEEE Computational Intelligence Society St. Louis chapter. He is currently an Associate Editor of the IEEE TRANSACTIONS ON EVOLUTIONARY COMPUTATION and an Editor of the IEEE TRANSACTIONS ON SMART GRID. He is a Fellow of the Institution of Engineering and Technology, U.K., and the South African Institute of Electrical Engineers. He was the recipient of several awards including the 2007 U.S. Office of Naval Research Young Investigator Program Award, the 2004 National Science Foundation CAREER Award, the 2010 Innovation Award from St. Louis Academy of Science, the 2010 IEEE Region 5 Outstanding Member Award, the 2005 IEEE Industry Applications Society Outstanding Young Member Award, a 2008, 2007, and 2005 Missouri S&T Faculty Excellence Award, and the 2009 Missouri S&T Faculty Research Award.



**Keith Corzine** (S'92–M'97–SM'06) received the B.S.E.E., M.S.E.E., and Ph.D. degrees from the University of Missouri, Rolla, in 1992, 1994, and 1997, respectively.

He was with the University of Wisconsin, Milwaukee, from 1997 to 2004, and is currently a Professor with the Missouri University of Science and Technology, Rolla. His research interests include power electronics, motor drives, naval ship propulsion systems, and electric machinery. He has published nearly 40 refereed journal papers, over

60 refereed international conference papers, and is the holder of three U.S. patents related to power conversion.

Dr. Corzine is currently the Industry Applications Society Chapter Chair and is on the Nomination and Appointments Committee of the IEEE St. Louis Section.